BIO-NANOPLATINUM PHYTO-DEVELOPED FROM GRAPE BERRIES AND NETTLE LEAVES: POTENTIAL ADJUVANTS IN OSTEOSARCOMA TREATMENT

M. E. BARBINTA-PATRASCU[1], M. BACALUM[2], V.A. ANTOHE[1,3], S. IFTIMIE[1], S. ANTOHE[1,4]*
[1]*University of Bucharest, Faculty of Physics, Department of Electricity, Solid-State Physics and Biophysics, 405 Atomistilor Street, PO Box MG-11, Bucharest-Magurele, 077125, Romania, E-mail: marcela.barbinta@unibuc.ro; vlad.antohe@fizica.unibuc.ro; sorina.iftimie@fizica.unibuc.ro; santohe@solid.fizica.unibuc.ro*
[2]*Horia Hulubei National Institute for Physics and Nuclear Engineering, Department of Life and Environmental Physics, Reactorului 30, 077125 Măgurele, Ilfov Romania; bmihaela@nipne.ro*
[3]*Université catholique de Louvain (UCLouvain), Institute of Condensed Matter and Nanosciences (IMCN), Place Croix du Sud 1, B-1348 Louvain-la-Neuve, Belgium; vlad.antohe@uclouvain.be*
[4]*Academy of Romanian Scientists, Ilfov Street 3, 050045 Bucharest, Romania; santohe@solid.fizica.unibuc.ro*

** Corresponding author: santohe@solid.fizica.unibuc.ro (S. ANTOHE)*

Abstract. Cancer remains the leading cause of millions of deaths annually, worldwide. Every year many people are diagnosed with osteosarcoma, the most common type of cancer starting in the bones. Recent advances in Green Nanotechnology are trying to fight against this disease. Thus, a special interest has been given to noble metal nanoparticles.

In this study, bio-platinum nanoparticles (bio-PtNPs) were generated through a "green" bottom-up approach, from an aqueous extract of a mixture of nettle leaves and grape berries. The obtained bio-PtNPs were analyzed by UV-Vis absorption spectroscopy, as well as by Scanning Electron Microscopy (SEM). These bio-PtNPs presented antiproliferative activity against MG-63 osteosarcoma cells, in a dose-dependent manner. The morphology of MG-63 cells treated with various doses of bio-PtNPs was studied by epifluorescence microscopy.

These findings could be exploited in the development of novel biohybrid systems to be used in osteosarcoma therapy.

Key words: "Green" platinum nanoparticles; osteosarcoma; antiproliferative activity

1. INTRODUCTION

Osteosarcoma represents almost 60% from the number of malignant primary bone cancers diagnosed in children and adolescents [1]. Osteosarcoma is a highly aggressive tumor, found in the long bones, which metastasizes firstly in lungs and pleurae [2] and is considered to have a higher occurrence in males than in females [3]. The most efficient treatment plans used at the moment are the combination of surgery with neoadjuvant and adjuvant chemotherapy [2]. However, for the patients suffering from advanced stages, who relapsed or have a strong side effect to chemotherapy, there are no efficient therapies.

Advances in modern nanotechnology, especially in Green Nanotechnology offered many advantages to overcome the drawbacks of conventional therapies in the osteosarcoma management. The nanomaterials bearing functional molecules

(e.g., antibodies, anti-cancer drugs, tumor-specific ligands, and imaging probes) are widely used for combating osteosarcoma progression [4]. An alternative to classical methods is related to the "green" strategies to fight against cancer, and one of them is the Green Nanotechnology that uses the principles of Green Chemistry for the preparation of nanomaterials with interesting properties. Plants and vegetal wastes represent valuable raw materials for Green Nanotechnology and they are increasingly used in last years for the synthesis of metal nanoparticles (MNPs) – the so-called *phytosynthesis* [5-7].

In this research, an aqueous extract containing mixture of nettle leaves and grape berries, was used to generate bio-platinum nanoparticles (bio-PtNPs). Our research group reported the "green" development of silver nanoparticles [8] and plasmonic biohybrids [9] with good biological performance (antioxidant, antibacterial and anticancer activities), starting from this plant mixture.

The vegetal resources mentioned above are rich in polyphenols and terpenoids [8, 10, 11], important bioactive molecules with antioxidant, antimicrobial and anticancer properties, which act as "electron shuttles" to bioreduce the metallic ions and also, act as capping agents for MNPs formation. Thus, many bioactive chemical constituents arising from plant extracts are on the surface of MNPs, and give them interesting properties such as antimicrobial activities, free radicals scavenging properties, and anticancer activity [1, 5-9, 12].

Platinum nanoparticles (PtNPs) obtained by eco-friendly approaches have superior physical and chemical properties and great potential in biomedical applications [12].

Platinum nanoparticles can induce cell cycle arrest, apoptosis and DNA breaks and are known to have a hemolytic effect at concentrations in the range of micromolar [1, 13-15].

The main objectives of our work were the following: i) valorization of vegetal resources/wastes to prepare bioactive nanomaterials; ii) the use of new trends in *Green Nanotechnology* for biosynthesis of platinum nanoparticles with interesting properties; iii) spectral and morphological characterization, and iv) evaluation of antiproliferative activity against osteosarcoma MG-63 cells.

2. MATERIALS AND METHODS

2.1. Materials

Hexachloroplatinic acid solution (H_2PtCl_6, 8 wt. % in H_2O; 409.81 g/mol) was purchased from Merck (Darmstadt, Germany). The vegetal materials were acquired from a local market. MTT (3-(4,5-dimethylthiazol-2-yl)-2,5-diphenyltetrazolium bromide) was purchased from Serva (Heidelberg, Germany) and dimethyl sulfoxide (DMSO) from Sigma Aldrich (Darmstadt, Germany). All cell cultivation media and reagents were purchased from Biochrome AG (Berlin, Germany).

2.2. Phyto-Synthesis of bio-PtNPs

Platinum nanoparticles (bio-PtNPs) were obtained from a mixture of two aqueous plant extracts: nettle (80% v/v) and of black grape berries (20% v/v). These vegetal extracts were prepared as previously described [8].

Bio-PtNPs were synthesized by mixing one volume of H_2PtCl_6 solution ($1.95 \cdot 10^{-4}$ M) with 9 volumes of the as prepared mixture plant extract. This suspension was kept in dark, under continuous stirring for 5h, at 55°C; the color of this suspension turned from yellow to dark brown, proving the formation of PtNPs.

The phytosynthesis of bio-PtNPs was initially observed by this color modification, and further confirmed by spectral and microscopic analyses.

2.3. Characterization methods of phyto-developed platinum nanoparticles

2.3.1 Spectral and morphological characterization of bio-PtNPs

The UV-Vis absorption spectra were recorded at room temperature, in ambient conditions, by using a double beam spectrophotometer Perkin Elmer Lambda 750, in the wavelength range of 200 - 800 nm; the scanning rate was 1 nm/s.

Morphological characterization of the samples was performed with a Tescan Vega-II Scanning Electron Microscope (SEM) operating in Secondary Electrons (SE) imaging mode. In this context, the samples were first thoroughly dried under normal environmental conditions for several hours and then they were carefully installed on the SEM holder using conducting carbon tape, used mainly to minimize specimen charging effects during the SEM observations.

2.3.2. Cell Culture

L929 cells (ATCC, Manassas, VA, USA) were grown in Minimal Essential Medium (MEM) supplemented with 2 mM L-Glutamine, 10% fetal calf serum (FCS) and 100 units/mL of penicillin and 100 µg/mL of streptomycin. MG-63 cells (ATCC, Manassas, VA, USA) were grown in MEM supplemented with 2 mM L-Glutamine, 10% FCS, 1% essential amino acids and 100 units/mL of penicillin and 100 µg/mL of streptomycin. All cell cultivation media and reagents were purchased from Biochrom AG (Berlin, Germany). Cells were kept in a humidified incubator at 37°C and 5% CO_2. For this study the cells were treated with different concentrations of nanoparticles for 24h.

2.3.3. Cell Viability

The biocompatibility of the biohybrids was evaluated using MTT tetrazolium reduction assay as follows. Cells were seeded in 96 well plates and cultured for 24h in medium. First, the cells were seeded into a 96 well plates at desired densities (7,000 cells/well for L929 cells, and 8,000 cells/well for MG-63 cells) and grown in medium for 24h before treatment with different concentrations of NPs for

additional 24h. Cells grown only in medium were used as negative control. Following incubation, the medium was changed and 1 mg/mL of MTT solution was added to each well and incubated for additional 4h at 37°C. Finally, the medium was collected and DMSO was used to dissolve the insoluble formazan product. The absorbance of the samples was recorded at 570 nm using a plate reader Mithras 940 (Berthold, Germany). The data were corrected for the background and the percentage of viable cells was obtained using the following equation:

$$\% \text{ Viable cells} = [(A_{570} \text{ of treated cells}) / (A_{570} \text{ untreated cells})] \cdot 100\% \quad (1)$$

The NP concentration that reduced the viability of the cells by half (IC_{50}) were obtained by fitting the data with a logistical sigmoidal equation using the software Origin 8.1 (Microcal Inc. U.S.A.). The therapeutic index (TI) was calculated as the ratio of the dose that produces toxicity to the dose needed to produce the desired therapeutic response [16].

2.3.4. Morphological evaluation of cells

Cells were grown on cover slips and treated for 24h with 0.82 μM for the biohybrids. Afterwards, the cells were washed with Phosphate-buffered saline (PBS), then fixed for 15 min with 3.7% formaldehyde dissolved in PBS, and washed again with PBS buffer. Sequentially, cells were stained with 20 μg/mL acridine orange (AO, Sigma-Aldrich, Darmstadt, Germany) solution for 15 min, then immediately washed with PBS, followed imaging using an Andor DSD2 Confocal Unit (Andor, Ireland), mounted on an epifluorescence microscope, Olympus BX-51 (Olympus, Germany), equipped with a 40x objective and an appropriate filter cube (excitation filter 466/40 nm, dichroic mirror 488 nm, and emission filter 525/54 nm).

2.3.5. Hemocompatibility

The hemolytic activity of the new hybrids was determined using an adapted protocol based on the ASTM F 756-00 standard previously described [16]. Briefly, fresh blood was collected on heparin from healthy volunteers and diluted with PBS to a final hemoglobin concentration of ~10 mg/mL. The blood was incubated with the highest concentration of the samples for 4h at 37ºC under constant shaking. Finally, the supernatant was collected and mixed with an equal amount of Drabkin reagent (Sigma-Aldrich). After 15 min, the absorbance of the samples was read at 570 nm using a plate reader. As negative and positive controls, the human red blood cells (hRBCs) in PBS and distilled water respectively, were used. The experimental values were corrected for background, dilution factors and used to calculate the percentage of hemolysis (i.e., hemolytic index), according to the equation:

$$\% \text{ Hemolysis} = (A_S / A_T)\ 100\ \% \quad (2)$$

Where, A_S is the corrected absorbance of the hemoglobin released in supernatant after treatment with nanoparticles and A_T is the corrected absorbance of the total released hemoglobin.

3. RESULTS AND DISCUSSIONS

3.1. Optical characterization of bio-developed nanoparticles

Bioreduction of platinum ions was firstly observed by visual inspection, finding the modification of the phyto-extract colour which turned from dark yellow to dark brown (Fig. 1, upper images), after addition of H_2PtCl_6, due to excitation of surface plasmon vibration in the platinum nanoparticles. The "green" synthesis of bio-nanoplatinum particles was demonstrated by the appearance of a strong absorption in UV region (Fig. 1, bottom images), which it was also observed by other researchers [17, 18]. These findings confirmed the phyto-reduction of Pt^{4+} ions to Pt^0 in nanoparticles.

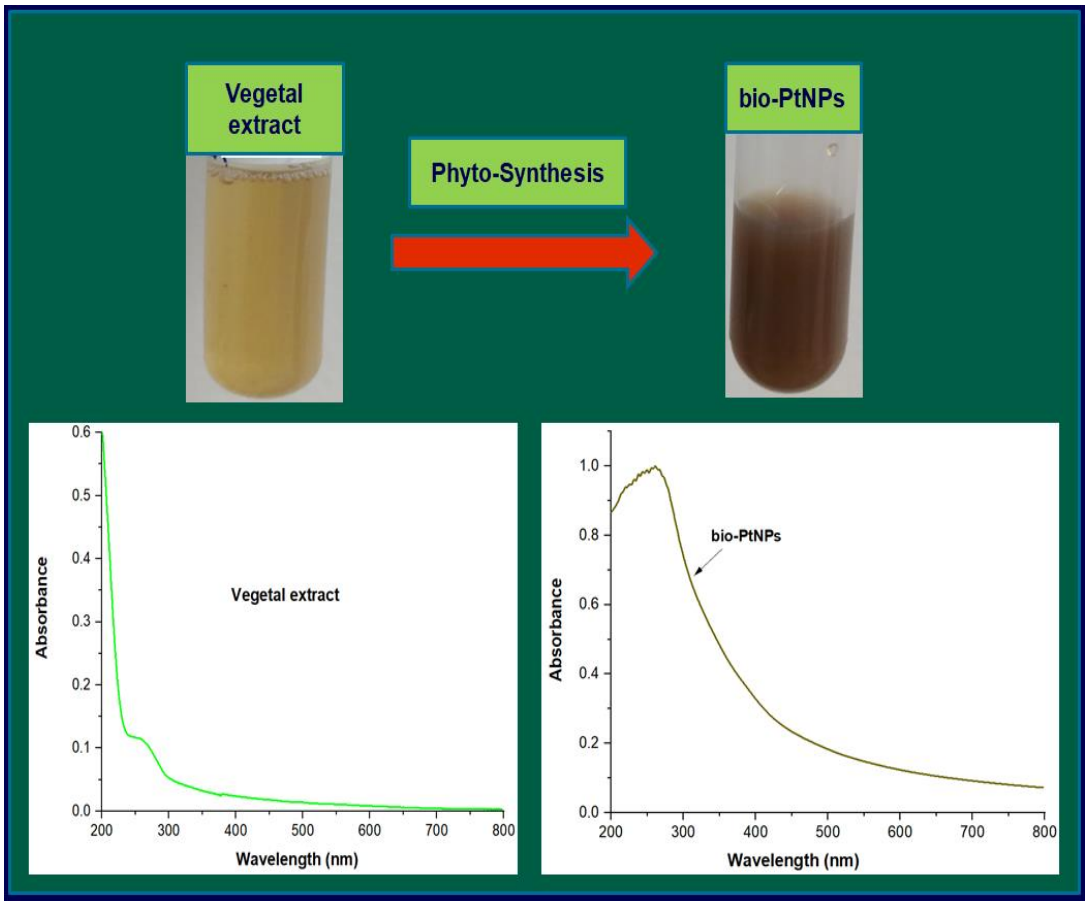

Fig. 1 – Visual inspection of the phytosynthesis of bio-PtNPs (upper images) and the comparative presentation of UV-Vis absorption spectra of the vegetal extract and of the synthesized bio-PtNPs (bottom images).

3.2. Morphological characterization of phytogenerated platinum nanoparticles

SEM micrographs (Fig.2) show the morphological aspects and the dimension of phyto-developed PtNPs. In the Fig.2a it could be observed the organic matrix arising from vegetal extract in which the bio-PtNPs are embedded. At a higher magnification (Fig.2b), it can be seen the quasi-spherical shape and the nanosize of the synthesized bio-PtNPs.

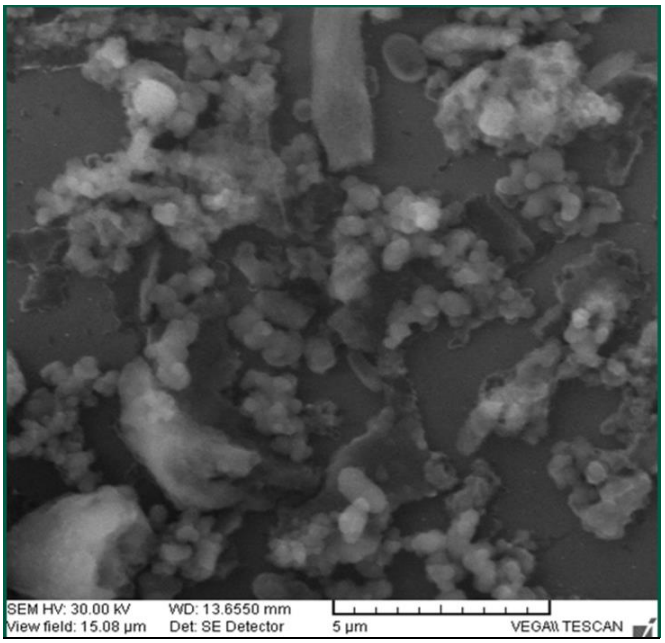

a)

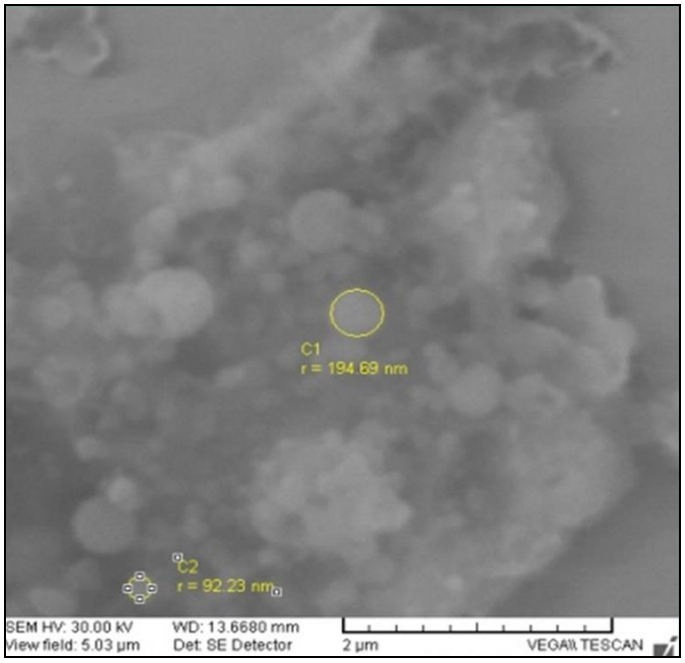

b)

Fig. 2 – SEM micrographs recorded for the synthesized bio-PtNPs at two magnifications.

3.3. Biological impact of bio-PtNPs

The bio-impact of phytosynthesized nano-platinum particles was evaluated by monitoring cell viability, cell morphology, and by calculating the hemolytic index and the therapeutic index.

In Figure 3 are presented the cell viability curves for L929 and MG-63 cell lines treated with various concentrations of PtNPs for 24h. One can see that at smaller concentrations (0.41 and 0.82 μM of bio-PtNPs), the cancerous MG-63 cells are more affected than the normal L929 cells, indicating that the NPs have an antitumor effect. For higher concentrations (above 0.82 μM of PtNPs), the NPs show similar toxicity for both normal and tumor cells.

The findings are in correlation with previous data reported. PtNPs showed their efficiency against human bone OS epithelial cells (U2OS) [1] and SH-SY5Y human neuroblastoma cells [19], in the range of 10-100 μg/mL.

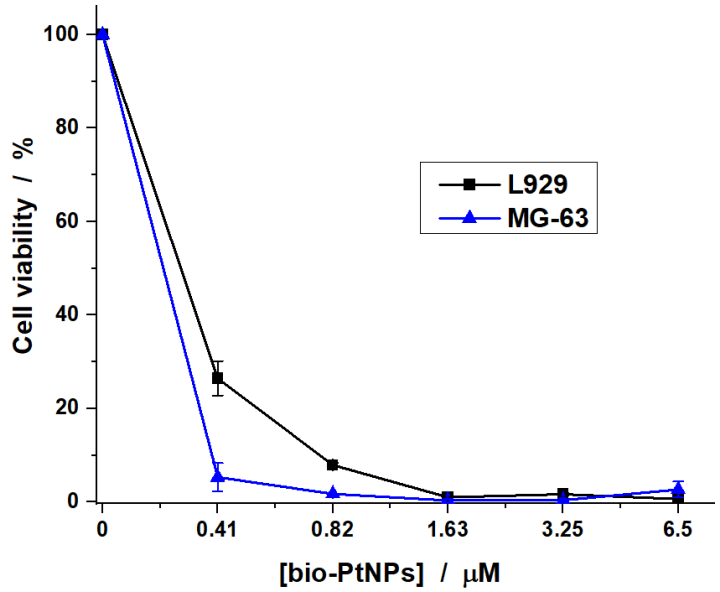

Fig. 3 – Cell viability after treatment with the phytosynthesized PtNPs for 24h.

Based on the viability curves we calculate the IC_{50} values, which are reported in Table 1. IC_{50} value found for L929 is 0.27 μM and for MG-63 is 0.21 μM. The TI value was 1.29, indicating that the obtained bio-PtNPs have higher affinity for MG-63 cells.

Morphological changes were investigated for cells treated with 0.82 μM and the results are presented in Figure 4. In Figure 4A we can see the untreated L929 cells which exhibit their normal morphology, a fusiform body with several branches. Contrary, when the bio-PtNPs are added (Figure 4B), we can see that the cells are drastically affected, as the size of the cell body is reduced and there are no more branches.

Similarly, for MG-63 cells, their morphology is drastically affected by the treatment with the synthesized bio-PtNPs. The untreated MG-63 cells (Figure 4C)

have a large body with some branches. When the treatment is added (Figure 4D), the size of the cell body is considerably reduced compared with the untreated cells, a greater effect than the one observed for L929 cells. The microscopy data confirm the results obtained for the viability studies, showing that at 0.82 μM the bio-PtNPs are affecting both the viability of the cells as well as their morphology, an effect more pronounced for the cancerous MG-63 cells than for the normal L929 cells.

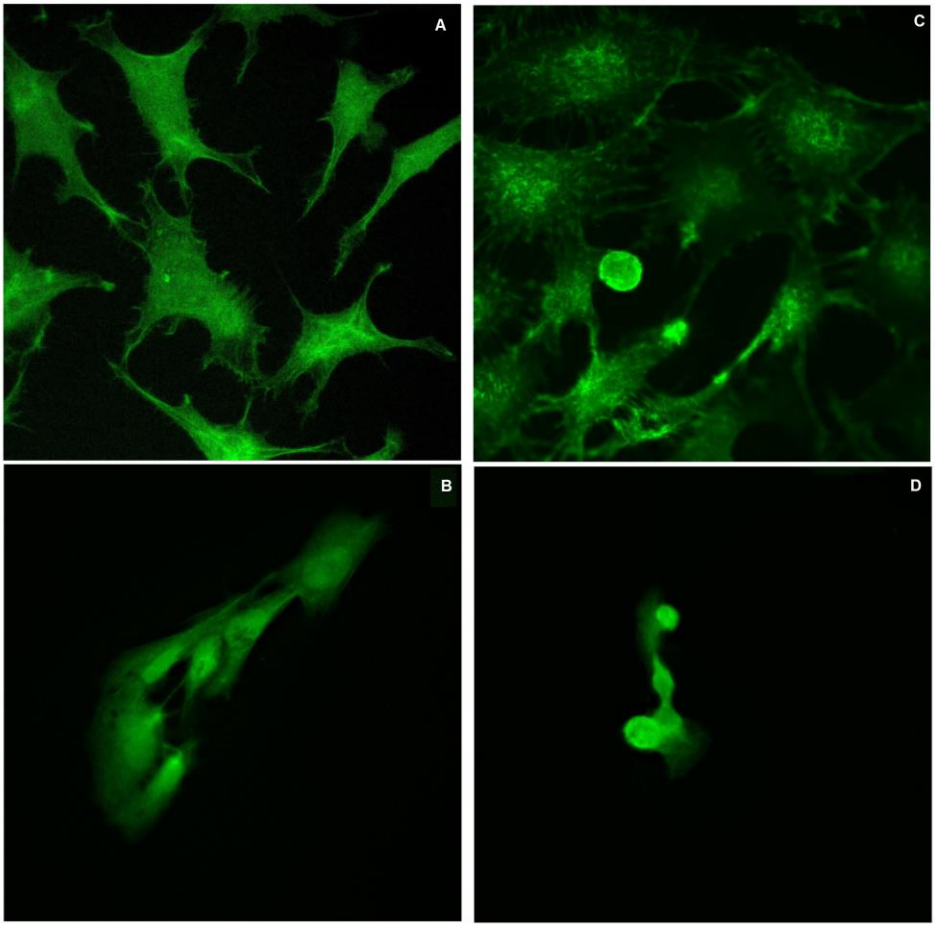

Fig. 4 – Morphology of L929 (A, B) and MG-63 (C, D) cells,
untreated and treated with 0.82 μM bio-PtNPs, respectively.
The images were obtained with the 40x objective and using the epifluorescence mode.

Furthermore, we also determined the hemolytic activity of our developed bio-PtNPs and the results are reported in Table 1. For a concentration of 0.82 μM, we found a percentage of hemolysis of 2%, which is indicative of a slight hemolytic effect. For higher concentrations, we found a hemolytic effect with index value of above 5%. The results are in accordance with data reported previously in the literature. Kutwin and collaborators have reported a strong hemolytic effect for both PtNPs (23%) and cisplatin (14%) at concentrations of 2.6 μg/mL (~13 μM) and 4 μg/mL, respectively [15].

Table 1

IC_{50} values, hemolytic index and therapeutic index (TI) found for the phytosynthesized PtNPs

	IC_{50} (μM)		**Hemolysis (%)**	**TI (μM)**
	L929	MG-63		MG-63
Bio-PtNPs	0.27	0.21	2% at 0.82 μM	1.29

4. Conclusions

This study described the phyto-generation of bio-nanoplatinum particles obtained from nettle and grapes mixture.

The SEM analysis highlighted the (quasi)spherical morphology and nanometric size of phytosynthesized platinum nanoparticles.

These phyto-designed nanoparticles showed an antiproliferative activity against osteosarcoma MG-63 cells, the therapeutic index value being 1.29.

A negligible hemolytic effect was detected for low NP doses (< 0.82 μM).

These findings are valuable for the development of novel "green" therapeutic nano-agents for osteosarcoma treatment.

Acknowledgements. This work was supported by the Project JINR–RO 2021 No. 38/2021 (IUCN Order 365/11.05.2021), by Romanian Ministry of Research, Innovation and Digitization, through the National Core Program No. PN 19 06 02 03/2019, as well as by the Executive Unit for Financing Higher Education, Research, Development and Innovation (UEFISCDI), through the grants: TE 115/2020 and TE 25/2020.

REFERENCES

1. S. Gurunathan, M. Jeyaraj, M.-H. Kang, J.-H. Kim, Nanomaterials **9**(8), 1089 (2019).
2. A. Longhi, C. Errani, M. De Paolis, M. Mercuri, G. Bacci, Cancer Treat. Rev. **32**(6), 423–436 (2006).
3. G. Ottaviani, N. Jaffe, The Epidemiology of Osteosarcoma. In: N. Jaffe, O. Bruland, S. Bielack (eds) Pediatric and Adolescent Osteosarcoma. Cancer Treatment and Research, vol 152. Springer, Boston, MA. https://doi.org/10.1007/978-1-4419-0284-9_1
4. M. Barani, M. Mukhtar, A. Rahdar, S. Sargazi, S. Pandey, M. Kang, Biosensors (Basel) **11**(2), 55 (2021).
5. I. Zgura, M. Enculescu, C. Istrate, R. Negrea, M. Bacalum, L. Nedelcu, M. E. Barbinta-Patrascu, Nanomaterials **10**(11), 2146 (2020).
6. M. E. Barbinta-Patrascu, J. Optoelectron. Adv. M. **22**(9-10), 523-528 (2020).
7. M. E. Barbinta-Patrascu, C. Ungureanu, D. Besliu, A. Lazea-Stoyanova, L. Iosif, Optoelectron. Adv. Mat. **14**(9-10), 459-465 (2020).
8. M. E. Barbinta-Patrascu, C. Nichita, N. Badea, C. Ungureanu, M. Bacalum, I. Zgura, L. Iosif, S. Antohe, Rom. Rep. Phys. **73**, 601 (2021).
9. Y. Gorshkova, M.-E. Barbinta-Patrascu, G. Bokuchava, N. Badea, C. Ungureanu, A. Lazea-Stoyanova, M. Răileanu, M. Bacalum, V. Turchenko, A. Zhigunov, E. Juszyńska-Gałązka, Nanomaterials **11**, 1811 (2021).
10. D. Kregiel, E. Pawlikowska, H. Antolak, Molecules **23**, 1664 (2018).
11. G. Gnanajobitha, K. Paulkumar, M. Vanaja, S. Rajeshkumar, C. Malarkodi, G. Annadurai, C. Kannan, J. Nanostructure Chem. **3**, 67 (2013).
12. S. A. Fahmy, E. Preis, U. Bakowsky, H. M. E.-S. Azzazy, Molecules **25**, 4981 (2020).

13. H. Gehrke, J. Pelka, C. G. Hartinger, H. Blank, F. Bleimund, R. Schneider, D.Gerthsen, S. Bräse, C. Marlene, M. Türk, D. Marko, Arch. Toxicol. **85**(7), 799–812 (2011).
14. M. Prasek, E. Sawosz, S. Jaworski, M. Grodzik, T. Ostaszewska, M. Kamaszewski, M. Wierzbicki, A. Chwalibog, Nanoscale Res. Lett. **8**(1), 251 (2013).
15. M. Kutwin, E. Sawosz, S. Jaworski, N. Kurantowicz, B. Strojny, A. Chwalibog, Nanoscale Res. Lett. **9**(1), 257 (2014).
16. M. E. Barbinta-Patrascu, N. Badea, M. Bacalum, C. Ungureanu, I. R. Suica-Bunghez, S. M. Iordache, C. Pirvu, I. Zgura, V. A. Maraloiu, Mat. Sci. Eng. C **101**, 120-137 (2019).
17. R. Dobrucka, Saudi J. Biol. Sci. **26**, 31–37 (2019).
18. A. Aygun,; F. Gülbagca, L.Y. Ozer, B. Ustaoglu, Y.C. Altunoglu, M.C. Baloglu, M.N. Atalar, M.H. Alma, F. Sen, J. Pharm. Biomed. Anal. **179**, 112961 (2020).
19. S. Gurunathan, M. Jeyaraj, M.-H. Kang, J.-H. Kim, Int. J. Mol. Sci. **21**, 6792 (2020).